

Supporting Information

Reitman et al. 10.1073/pnas.1019393108

SI Results

BCAAs. In addition to alterations in amino acids and TCA metabolites detailed in the main text, we also noted changes in the BCAAs valine, leucine, and isoleucine, as well as intermediates in their breakdown (Fig. 4C). Leucine, isoleucine, and valine were higher in all three groups (range: 1.4- to 3.0-fold; $P < 0.05$ for all nine comparisons). The branched-chain α -keto acids 4-methyl-2-oxopentanoate, 3-methyl-2-oxovalerate, and 3-methyl-2-oxobutyrate can be converted directly from valine, leucine, and isoleucine, respectively, and are intermediates in their degradation. We found that 4-methyl-2-oxopentanoate and 3-methyl-2-oxopentanoate were elevated in IDH2-R172K-expressing cells and 2HG-treated cells (range: 1.5- to 2.5-fold; $P < 0.03$ for all four comparisons) and tended to be elevated in IDH1-R132H-expressing cells (1.7- and 1.4-fold; $P < 0.10$ for both comparisons). At the same time, 4-methyl-2-oxopentanoate, 3-methyl-2-oxovalerate, and 3-methyl-2-oxobutyrate were all decreased by more than twofold in culture medium incubated with cells expressing IDH1-R132H ($P < 0.03$). Although BCAA and branched-chain α -keto acids were elevated in cells expressing IDH mutants and cells treated with 30 mM 2HG, further downstream metabolites of BCAA breakdown were lowered in these cells. These metabolites include isobutyrylcarnitine, isovalerylcarnitine, and 2-methylbutyrylcarnitine (range: 2.5- to 7.7-fold; $P < 0.005$ for all nine comparisons).

Choline Lipid Metabolites. IDH mutant expression and 2HG treatment also resulted in alterations of choline lipid synthesis intermediates. In this pathway, choline is converted to choline phosphate, then to cytidine-5'-diphosphocholine (CDP-choline), and then to GPC (Fig. 4D), which serves as a precursor for membrane choline phospholipids. Remarkably, choline phosphate was 10-fold lower in IDH1-R132H-expressing cells, 1.8-fold lower in IDH2-R172K-expressing cells, and 100-fold lower in cells treated with 30 mM 2HG ($P < 0.001$ for each). Conversely, GPC was higher in IDH1-R132H- (1.9-fold; $P < 0.001$) and 2HG-treated (3.0-fold; $P < 0.001$) cells, respectively, although it was decreased in IDH2-R172K cells (1.3-fold; $P = 0.04$). GPC also was 1.9-fold elevated in culture medium incubated with IDH1-R132H cells ($P = 0.04$; Fig. S3D).

SI Materials and Methods

Cell Lines. Human oligodendroglioma (HOG) cells were derived from a human WHO grade III anaplastic oligodendroglioma (1) and previously found not to contain exon 4 isocitrate dehydrogenase 1 (IDH1) or exon 4 isocitrate dehydrogenase 2 (IDH2) mutations (2). The HOG cell line was kindly donated by A. T. Campagnoni (University of California, Los Angeles). To express IDH1 and IDH2 transgenes in cells, IDH1 and IDH2 cDNAs or cDNAs mutagenized to IDH1-R132H or IDH2-R172K were cloned into pLenti6.2/V5 (Invitrogen). Viruses were created using these constructs in 293FT cells and were used to transduce cells derived from the same parental pool of HOG cells for 24 h. Cells derived from the same clone were reasoned to have homogenous IDH transgene expression levels and metabolic profiles compared with pools of cells or transiently transfected cells, facilitating the identification of metabolites that have altered levels in different clones. Virus was replaced by fresh medium for 48 h, and then stable clones were selected from single-cell dilutions in 5 μ g/mL blasticidin for 3 wk. The same clones of vector, IDH1-WT, and IDH1-R132H HOG cells were used in all experiments.

(R)-2-hydroxyglutarate Synthesis. (R)-2-hydroxyglutarate (2HG) was synthesized by treatment of D-glutamate (Sigma-Aldrich) with nitrous acid to form a lactone, which was then hydrolyzed with NaOH solution to form 2-D-hydroxyglutarate. Purity was 93%. Powder was resuspended in PBS and filtered through a 0.22- μ m filter using sterile technique for treatment of cells.

Metabolomic Analysis. Cell line treatment. Cells were grown under respective experimental conditions in Iscove's Modified Dulbecco's Medium (IMDM) (Gibco, Invitrogen) supplemented with 10% FBS. For the experiment in Fig. 2, cells were grown in a medium mix that also contained 10% PBS or 10% of a 300-mM or 75-mM 2HG solution in PBS for a final 30 mM or 7.5m M 2HG. Cells were seeded into flasks 3 d before harvesting. To harvest cells, medium was removed, monolayers were washed with PBS, and 0.05% trypsin/EDTA was added. Cells were incubated for 20 min at 37 °C or until cells detached. Two volumes of medium were added to the Trypsin/cell mix and suspended by gentle pipetting and titration. Cells were counted, and 10^7 cells per sample were spun down at $300 \times g$ for 3 min in a polystyrene tube. Cells were washed twice with PBS and then snap-frozen on dry ice and stored at -80 °C until analysis.

Metabolite analysis. Metabolomic profiling analysis of all samples was carried out in collaboration with Metabolon as described previously (3–5).

Sample accessioning. Each sample received was accessioned into the Metabolon Laboratory Information Management System (LIMS) and was assigned a unique identifier associated only with the original source identifier. This identifier was used to track all sample handling, tasks, results, and other data. The samples (and all derived aliquots) were bar-coded and tracked by the LIMS system. All portions of any sample were automatically assigned unique identifiers by the LIMS when a new task was created; the relationship of these samples was tracked also. All samples were maintained at -80 °C until processed.

Sample preparation. The sample preparation process was carried out using the automated MicroLabSTAR system (Hamilton Company). Recovery standards were added before the first step in the extraction process for quality control (QC) purposes. Sample preparation was conducted using a proprietary series of organic and aqueous extractions to remove the protein fraction while allowing maximum recovery of small molecules. The resulting extract was divided into two fractions, one for analysis by liquid chromatography (LC) and one for analysis by gas chromatography (GC). Samples were placed briefly on a TurboVap (Zymark) to remove the organic solvent. Each sample then was frozen and dried under vacuum. Samples were then prepared for the appropriate instrument, either LC-MS or GC-MS.

Quality assurance/QC. For quality assurance (QA)/QC purposes, additional samples were included with each day's analysis. These samples included a well-characterized pool of human plasma, a pool of a small aliquot of each experimental sample, an ultra-pure water process blank, and an aliquot of solvents used in extraction to segregate contamination sources in the extraction. Furthermore, a selection of QC compounds was added to every sample, including those under test. These compounds were chosen carefully so as not to interfere with the measurement of the endogenous compounds.

LC-MS and LC-MS/MS. The LC-MS portion of the platform was based on an ACQUITY ultra-performance liquid chromatography (UPLC) system (Waters) and an linear trap quadrupole (LTO) mass spectrometer (Thermo-Finnigan), which consisted of an electrospray ionization (ESI) source and linear ion-trap (LIT) mass analyzer. The sample extract was split into two aliquots, dried,

and then reconstituted in acidic or basic LC-compatible solvents, each of which contained 11 or more injection standards at fixed concentrations. One aliquot was analyzed using acidic positive ion-optimized conditions and the other using basic negative ion-optimized conditions in two independent injections using separate dedicated columns. Extracts reconstituted in acidic conditions were gradient eluted using water and methanol, both containing 0.1% formic acid. The basic extracts, which also used water/methanol, contained 6.5 mM ammonium bicarbonate. The MS analysis alternated between MS and data-dependent MS/MS scans using dynamic exclusion.

GC-MS. The samples destined for GC-MS analysis were redried under vacuum desiccation for a minimum of 24 h before being derivatized under dried nitrogen using Bis(trimethylsilyl)trifluoroacetamide (BSTFA). The GC column was 5% phenyl, and the temperature ramp was from 40° to 300 °C in a 16-min period. Samples were analyzed on a Thermo-Finnigan Trace DSQ fast-scanning single-quadrupole mass spectrometer using electron-impact ionization. The instrument was tuned and calibrated for mass resolution and mass accuracy on a daily basis. The information output from the raw data files was extracted automatically as discussed below.

Accurate mass determination and MS/MS fragmentation. The LC-MS portion of the platform was based on a Waters ACQUITY UPLC and a Thermo-Finnigan LTQ-FT mass spectrometer, which had an LIT front end and a Fourier transform ion cyclotron resonance (FT-ICR) mass spectrometer back end. For ions with counts greater than 2 million, an accurate mass measurement could be performed. Accurate mass measurements could be made on the parent ion as well as on fragments. The typical mass error was less than 5 ppm. Ions with less than 2 million counts require more effort to characterize. Fragmentation spectra (MS/MS) typically were generated in a data-dependent manner, but, if necessary, targeted MS/MS could be used, as was done with lower-level signals.

Number of biochemicals detected. At the time of publication, the metabolomics platform is capable of detecting ~10,000 unique biochemicals, including 2,200 known metabolites and the remainder consisting of unique metabolites of unknown structure. As discussed below, only metabolites present at levels within the range of quantification for a sufficiently large proportion of samples within a batch of samples were analyzed for that batch. **Instrument and process variability.** Confounding factors related to technical differences in the behavior of the LC-MS/MS or GC-MS/MS in each sample run (instrumental variability) and to differences in the preparation of individual samples (process variability) inevitably result in differences between samples that are unrelated to the biological variable of interest (i.e., 2HG treatment or transgene expression). To provide information on instrument variability, internal standards were added to each sample before injection into the mass spectrometers. Then, the median relative SD (RSD) of the ion counts of these standards for all samples in each batch was calculated. Information on overall process variability was provided by calculating the median RSD for all endogenous metabolites (i.e., noninstrument standards) present in 100% of the cell lysate samples in each batch. The median RSD values for the batch of HOG cell lysates expressing IDH1 and IDH2 transgenes (Fig. 1 and [Dataset S1](#)) were 6% for internal standards and 12% for endogenous metabolites. Median RSD values for the batch of spent medium samples ([Fig. S3](#) and [Dataset S2](#)) were 4% for internal standards and 10% for endogenous metabolites. Median RSD values for the batch of HOG cell lysates expressing IDH1-R132H, treated with 2HG or with IDH1 knockdown ([Fig. 2](#) and [Dataset S3](#)) were 6% for internal standards and 14% for endogenous metabolites.

Agreement between sample runs. One hundred seventy-nine of the biochemicals detected and analyzed in the first cell lysate metabolomic analysis ([Fig. 1](#) and [Dataset S1](#)) also were detected and analyzed in the second cell lysate metabolomic analysis ([Fig. 2](#) and [Dataset S3](#)). Some biochemicals were detected in one run and not another because variations in the lower limit of detection in dif-

ferent runs. Of these 179 biochemicals, 118 were significantly changed ($P < 0.05$) in IDH1-R132H-expressing cells in at least one experiment. One hundred of these biochemicals were changed in the same direction in both experiments, and three biochemicals were significantly changed in opposite directions in the two experiments.

Targeted Mass LC-MS/MS. Simultaneous quantification of *N*-acetyl-aspartate (NAA) and *N*-acetyl-aspartyl-glutamate (NAAG) in cell culture medium, cell lysates, and tissues was done by LC-ESI-MS/MS.

Materials. NAA and NAAG were from Sigma-Aldrich. Reagents and solvents were of analytical grade. Chromatography solvents were of LC-MS grade.

Sample preparation. Media above the cells and cell lysates. To 20 μ L of sample 40 μ L of ice-cold methanol was added. The mixture was vigorously agitated (speed 6, FastPrep; Qbiogene) for 20 s, left at -20 °C for 15 min, agitated again under the same conditions, and centrifuged at $16,000 \times g$ for 5 min. Then 50 μ L of supernatant was dried by vacuum centrifuge (SpeedVac; Thermo Scientific) at 50 °C for 1 h. The dry residue was dissolved by 50 μ L of mobile phase A (see below), and 10 μ L was injected into the LC-MS/MS system. **Tissue samples.** To a 10- to 50- μ g sample of wet tissue, 300 μ L of deionized water and one 4-mm ceramic bead were added in a 2-mL polypropylene tube and agitated vigorously (speed 4, FastPrep) for two 20-s cycles. A 50- μ L aliquot of the homogenate was pipetted out for total protein measurement (for tissue mass normalization purposes), and 500 μ L of methanol was added to the original vial, which was agitated again under the same conditions, left at -20 °C for 15 min, and centrifuged at $16,000 \times g$ for 5 min. Then 650 μ L of supernatant was dried by vacuum centrifuge (SpeedVac,) at 50 °C for 1.5 h. The dry residue was dissolved by 50 μ L of mobile phase A (see below), and 10 μ L was injected into the LC-MS/MS system.

LC-MS/MS analysis. For LC-MS/MS analysis, we used an Agilent 1200 series HPLC and Sciex/Applied Biosystems API 3200 QTrap. For mobile phase A, we used water, 3% methanol; for mobile phase B, we used acetonitrile/methanol in a ratio of 1:1. The analytical column was Kinetex C₁₈, 150 \times 4.6 mm, 2.6 μ m; the guard column was a SafeGuard C₁₈ 4 \times 3 mm guard column from Phenomenex. The column temperature was 45 °C. The elution gradient at a flow rate of 1 mL/min was 0–1 min 0% B, 1–2 min 0–80% B, 2–3.5 min 80% B, 3.5–4 min 80–0% B, 4–10 min 0% B. Injection volume was 10 μ L. The Q1/Q3 (*m/z*) transitions monitored in positive ESI mode were 176/158 (NAA, quantification), 176/134 (NAA, confirmation), 305/148 (NAAG, quantification), and 305/130 (NAAG, confirmation).

Calibration. A set of samples in corresponding matrix was prepared for calibration by adding appropriate amounts of pure NAA and NAAG at the following concentration levels: 0, 0.01, 0.05, 0.25, 1.25, and 6.25 μ g/mL. These samples were analyzed alongside the experimental samples; accuracy acceptance criterion was 85% for each except at the lowest level (0.01 μ g/mL, 80%). The limit of quantification (at the 80% accuracy criterion) was determined to be 10 ng/mL for both NAA and NAAG. Samples in which NAA or NAAG was not detected were assigned a value of 0 NAA or 0 NAAG ([Fig. 5 A](#) and [B](#)). Statistically significant differences that we reported ([Fig. 5 A](#) and [B](#)) remained significant when 10 ng/mL was set as the limit for detection of NAA or NAAG. Quadratic least squares regression curve fit was used to account for slight but predictable nonlinearity (ESI of highly polar analytes) with 1/x weighing factor. A recently reported method of NAAG analysis (6) also adds methanol to the sample matrix.

Glioma Tissue. Glioma samples were obtained from the Preston Robert Tisch Brain Tumor Center Biorepository at Duke University. Samples were selected based on tissue availability. Samples were analyzed previously for tumor type and IDH mutation status

by sequencing exon 4 of IDH1 and exon 4 of IDH2 (2). Samples listed as WT had no mutations of either IDH1 or IDH2 in exon 4. Tissue was dissected carefully by cutting 3- to 5-mg samples from frozen blocks on dry ice.

Statistics. Imputation and normalization. Some biochemicals were detected in some, but not all, samples in an experiment. Biochemicals that were detected in <50% of replicates in a study group were not analyzed further. Biochemicals that were detected in all samples from one or more groups but not in samples from other groups were assumed to be near the lower limit of detection in the groups in which they were not detected. In this case, the lowest detected level of these biochemicals was imputed for samples in which that biochemical was not detected. Quantification values then were normalized to protein concentrations obtained using the Bradford assay. Biochemicals were mapped to pathways based on KEGG, release 41.1 (<http://www.genome.jp/kegg>) (7). We did not include 2-oleoylglycerol (2-monoolein) in statistical analyses because it was detected in only one of 30 samples in experiment 2.

Univariate statistics. Welch's *t* test was used to determine whether mean levels of a biochemical in one experimental group differed from mean levels in another group. The *Q* value estimates the likelihood that a statistically significant comparison is a false discovery (8). *Q* values for each comparison are shown in **Datasets S1, S2, and S3**. For this study, comparisons with $P < 0.05$, $Q < 0.01$ would be estimated to have a false-discovery rate <1%. The *Q* values are listed in the **Datasets S1, S2, and S3** to provide additional information about changes in biochemical abundances, but *Q* values were not a criterion for the analyses described here. A two-tailed Student's *t* test assuming unequal variances was used to determine whether samples differed in NAA or NAAG levels (Fig. 5A). NAA and NAAG measurements in lysates and spent media are from four LC-MS/MS readings on two independent experiments and are representative of six LC-MS/MS readings on three independent experiments (Fig. 5A and B). A one-tailed Student's *t* test assuming equal variances was used to determine whether relative mean levels of NAA or NAAG in tumor tissue were significantly lower for tumors with IDH1 mutations than for tumors without IDH1 or IDH2 mutations (**Dataset S3**, Tumor NAA_NAAG tab).

Multivariate statistics. Multivariate statistics and associated graphics were performed in R, version 2.12.2 (9). Pearson product-moment correlation coefficients (*r*) were calculated using the *cor* function (**Tables S1 and S2**). For heat maps (Figs. 1A and 2A and Fig. S3A), Pearson distance was used as the pairwise distance between individual replicates. Pearson distance was calculated as $1 - r$. Dendrograms were created from this pairwise distance data using the

as.dist function, hclust (complete linkage method) function, and as.dendrogram function. Heat maps were drawn using these dendrograms and the heatmap.2 function found in the gplots package. Heat maps of *z* scores (Figs. 1A and 2A and Fig. S3A) and fold-changes (Figs. 3 and 4 and Fig. S3D) were plotted using log₂-transformed data. However, the color keys indicate the actual (non-log₂-transformed) values. Principal component analysis (PCA) was performed using the prcomp function (Figs. 1C and 2C and Figs. S1E and F, S3C, and S4B and C). For fold-change of IDH1-R132H cells, the average value from two independent experiments is displayed (Figs. 3 and 4).

Removal of outliers. We detected three outlier biochemicals with extremely different values from sample to sample that tended (i) to mask the effects of other biochemicals and (ii) to exaggerate the similarity that we observed in the IDH1-R132H, IDH2-R172K, and 2HG-treatment groups. We identified outlier biochemicals as biochemicals that clustered in a separate branch from all other biochemicals in unsupervised hierarchical clustering, had a PCA loading value more than twice as high as other biochemicals, and had a more than fivefold difference in absolute value between at least two samples. To display the complexity of these data better, we removed several such outliers based on these criteria. For this reason 2HG was removed from all heat maps, PCA, and Pearson correlation calculations (Figs. 1 and 2, Figs. S1, S3, and S4, and **Tables S1 and S2**). In the dataset derived from spent media samples (**Dataset S2**), pyrophosphate and methyl-4-hydroxybenzoate also met our criteria for outliers. Also, both metabolites had spurious MS readings in different replicates within several of the sample groups (**Dataset S2**). Both of these metabolites were removed from analyses of these data (Fig. S3).

Notes on Datasets. For **Datasets S1, S2, and S3**, the RawData tab contains ion counts from MS analysis associated with each biochemical. NA indicates the biochemical was not detected in that sample. The NormImpData tab contains raw ion count data that have been normalized by protein concentration, with each biochemical rescaled to have a median equal to 1 and missing values imputed with the minimum. The Heatmap tab organizes biochemicals mapped to their respective biochemical pathway and superpathway based on the Kyoto Encyclopedia of Genes and Genomes (KEGG). It includes mean relative abundance data, mean-to-mean comparisons of the abundance of each biochemical, and *P*-value and *Q*-value information from Welch's *t* test comparisons. The detection method (LC-MS/MS positive or negative ESI or GC-MS), Metabolon compound ID, KEGG, and Human Metabolome Database (HMDB), version 2.5, (<http://www.hmdb.ca/>) IDs, percent filled values, and compound mass are included also.

1. Post GR, Dawson G (1992) Characterization of a cell line derived from a human oligodendroglioma. *Mol Chem Neuropathol* 16:303–317.
2. Yan H, et al. (2009) IDH1 and IDH2 mutations in gliomas. *N Engl J Med* 360:765–773.
3. Ryals J, Lawton K, Stevens D, Milburn M (2007) Metabolon, Inc. *Pharmacogenomics* 8: 863–866.
4. Lawton KA, et al. (2008) Analysis of the adult human plasma metabolome. *Pharmacogenomics* 9:383–397.
5. Evans AM, DeHaven CD, Barrett T, Mitchell M, Milgram E (2009) Integrated, nontargeted ultrahigh performance liquid chromatography/electrospray ionization tandem mass spectrometry platform for the identification and relative quantification of the small-molecule complement of biological systems. *Anal Chem* 81:6656–6667.
6. Thomas AG, Rojas CJ, Hill JR, Shaw M, Slusher BS (2010) Bioanalysis of N-acetyl-aspartyl-glutamate as a marker of glutamate carboxypeptidase II inhibition. *Anal Biochem* 404: 94–96.
7. Kanehisa M (2009) Representation and analysis of molecular networks involving diseases and drugs. *Genome Inform* 23:212–213.
8. Storey JD, Tibshirani R (2003) Statistical significance for genomewide studies. *Proc Natl Acad Sci USA* 100:9440–9445.
9. R Development Core Team (2008) *R: A Language and Environment for Statistical Computing* (R Foundation for Statistical Computing, Vienna).

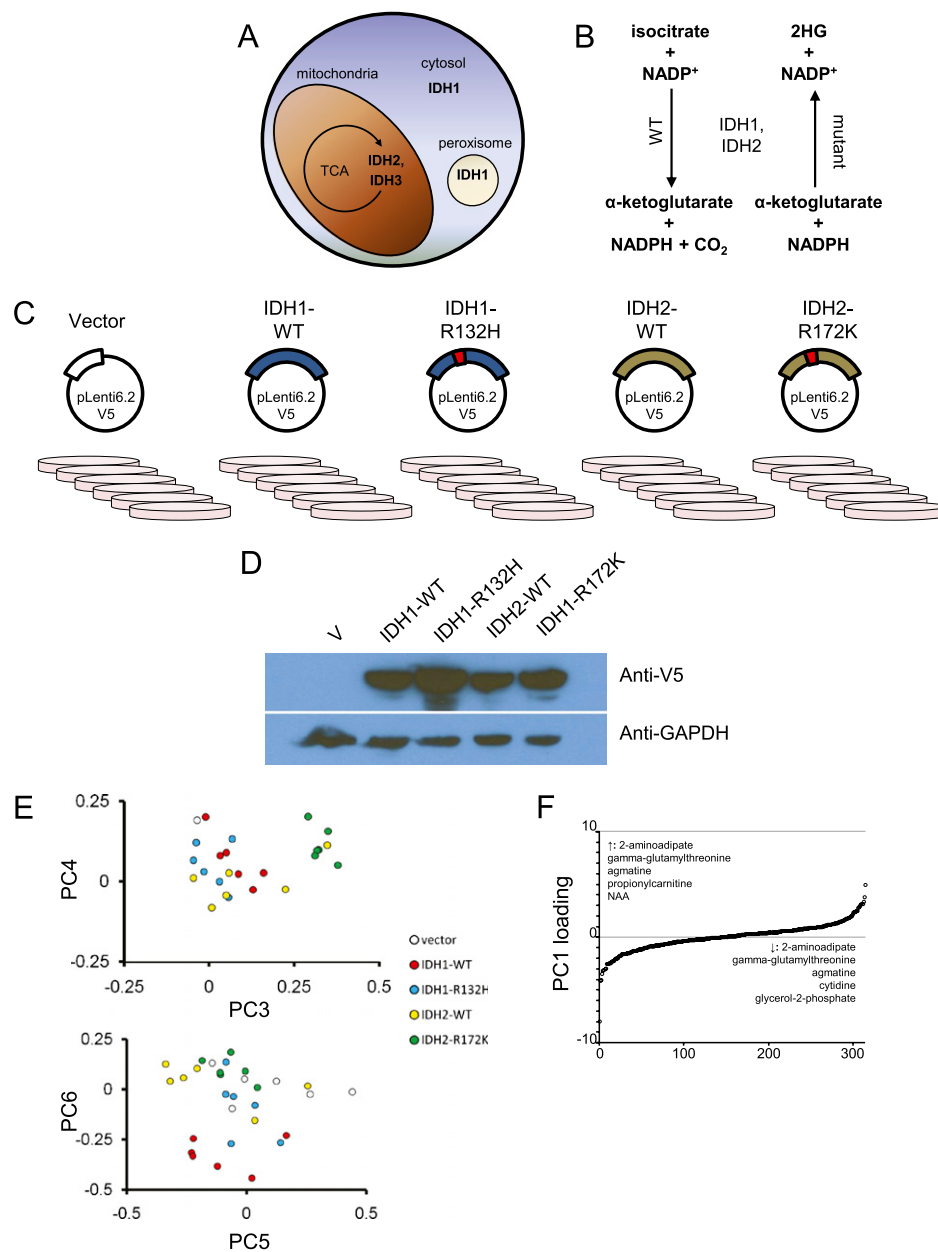


Fig S1. Overview, validation, and additional data for metabolomic analysis of HOG cells expressing IDH1 and IDH2 transgenes. (A) Normal cellular localization of the isocitrate dehydrogenases IDH1, IDH2, and IDH3. (B) Enzymatic function of WT IDH1 and IDH2 and of cancer-derived IDH1 and IDH2 mutants such as IDH1-R132H and IDH2-R172K. (C) Five clones of HOG cells were stably transduced with a lentivirus vector to express different transgenes. The transgenes include IDH1-WT, IDH1-R132H, IDH2-WT, IDH2-R172K, and an empty vector (V) control. Six replicate samples of each group were grown for analysis (Dataset S1). (D) Anti-V5 and anti-GAPDH immunoblot of HOG clones described in C. (E) Plots of principal component 3 (PC3)–PC6 from PCA analysis of replicate samples from C. (F) PC1 loading values for 314 biochemicals, arranged in order of increasing loading value. The five biochemicals with the highest and lowest loading values are listed.

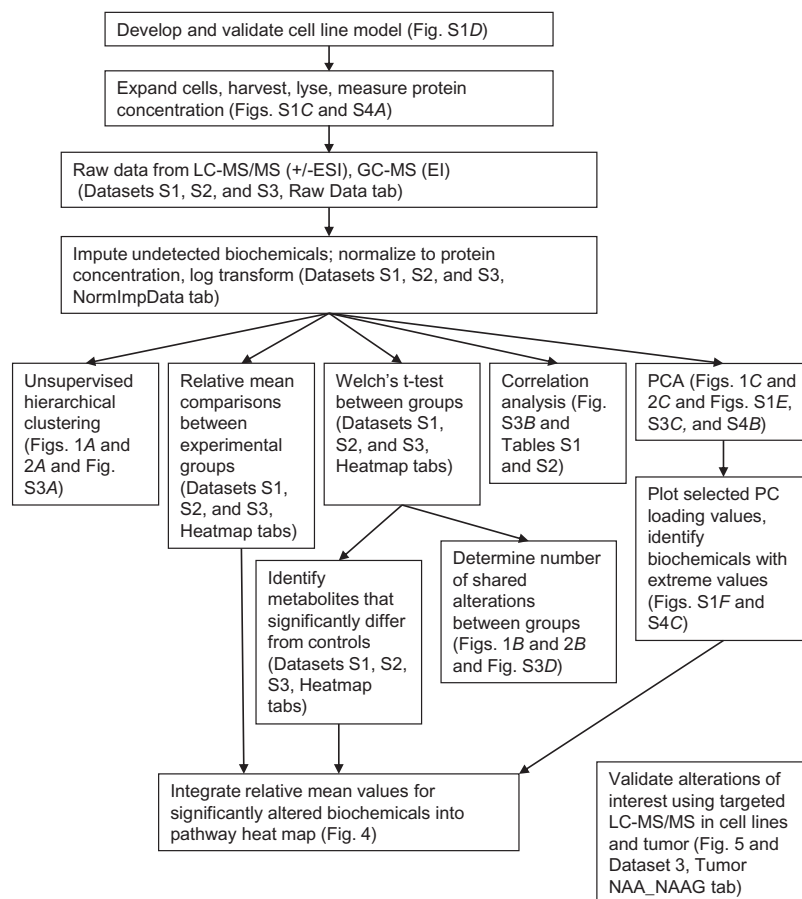


Fig S2. Summary of technical and statistical methods used in metabolomic profiling experiments in this study. Samples were generated from a human glioma cell line as described in the text and analyzed by LC-MS/MS (with or without ESI) and GC-MS [with electron-impact ionization (EI)]. Then they were subjected to multivariate and univariate statistical analyses to identify global and specific metabolite differences in different transgene expression and experimental treatment groups as shown.

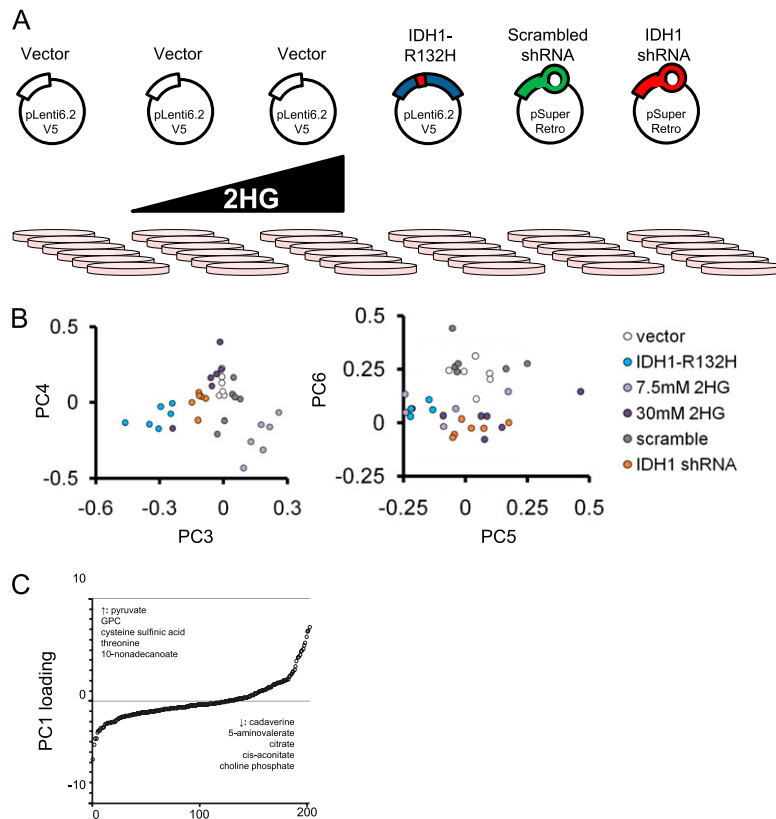


Fig S4. Overview and additional data for metabolomic analysis of HOG cells expressing IDH1-R132H, with IDH1 knockdown, or with 2HG treatment. (A) The following types of cells were analyzed: vector, (without treatment) or treated with 7.5 mM or 30 mM 2HG, cells expressing IDH1-R132H, cells expressing shRNA targeted to IDH1, and cells expressing scrambled control shRNA. (B) Plots of PC5–PC8 from PCA analysis of replicate samples of six HOG cell treatments (Dataset S3). (C) PC1 loading values for 202 biochemicals, arranged in order of increasing loading value. The five biochemicals with the highest and lowest loading values for PC1 are listed.

Table S1. Correlation between metabolite levels in HOG cells expressing IDH1 and IDH2 transgenes

	Vector	IDH1-WT	IDH1-R132H	IDH2-WT
IDH1-WT	$r = 0.048, P = 0.397$			
IDH1-R132H	$r = -0.249, P < 10^{-5}$	$r = -0.412, P < 10^{-6}$		
IDH2-WT	$r = 0.147, P < 0.001$	$r = 0.189, P < 0.001$	$r = -0.313, P < 10^{-6}$	
IDH2-R172K	$r = -0.218, P < 10^{-4}$	$r = 0.097, P < 0.086$	$r = 0.149, P < 0.008$	$r = -0.371, P < 10^{-6}$

Pearson product moment correlation coefficient (r) between mean biochemical abundances in HOG cells expressing IDH1-R132H, IDH2-R172K, or IDH1-WT, IDH2-WT, and vector controls (Dataset 1). Two-tailed P value is shown also.

Table S2. Correlation between metabolite levels in HOG cells expressing IDH1-R132H, with IDH1 knockdown, or with 2HG treatment

	Vector	IDH1-R132H	7.5m M 2HG	30mM 2HG	scramble
IDH1-R132H	$r = -0.169, P = 0.016$				
7.5 mM 2HG	$r = -0.400, P < 10^{-6}$	$r = -0.008, P = 0.910$			
30 mM 2HG	$r = -0.349, P < 10^{-6}$	$r = 0.225, P = 0.001$	$r = 0.542, P < 10^{-6}$		
Scrambled	$r = 0.377, P < 10^{-6}$	$r = -0.204, P = 0.003$	$r = -0.170, P = 0.015$	$r = -0.361, P < 10^{-6}$	
IDH1 shRNA	$r = 0.229, P < 0.001$	$r = -0.152, P = 0.030$	$r = -0.026, P = 0.712$	$r = -0.233, P < 0.001$	$r = 0.130, P = 0.064$

Pearson product moment correlation coefficient (r) between mean biochemical abundances in cells expressing IDH1-R132H, expressing IDH1 shRNA, or treated with 2HG (Dataset 3). Two-tailed P value is shown also.

Dataset S1. Metabolomic analysis of clonal HOG cells expressing IDH1 and IDH2 transgenes

[Dataset S1](#)

This dataset contains information on the abundance of 315 biochemicals for six replicates each of cleared lysates of clonal HOG cells that stably express one of four transgenes or that were treated with a vector control. Experimental groups include empty vector control (EV), IDH1-WT expression, IDH1-R132H expression, IDH2-WT expression, and IDH2-R172K expression. One hundred unique biochemicals with unknown identity are included and are designated as "X-#."

Dataset S2. Metabolomic analysis of spent media incubated with HOG cells expressing IDH1-R132H, IDH1-WT, or empty vector

[Dataset S2](#)

This dataset contains abundance data for 114 biochemicals from MS analysis of three replicates each of IMDM medium that was incubated above HOG cells for 48 h. In this dataset, one-way ANOVAs are included also, and data also are displayed as boxplots for each biochemical in the Boxplots tabs.

Dataset S3. Metabolomic analysis of HOG cells expressing IDH1-R132H, with IDH1 knockdown, or with 2HG treatment

[Dataset S3](#)

This dataset contains abundance data for 204 biochemicals from MS analysis of six replicates each of HOG cells from six experimental transgene expression or 2HG-treatment groups. Groups include vector, vector incubated in medium containing 7.5 mM 2HG (2HG low), vector incubated in 30 mM 2HG medium (2HG high), cells expressing IDH1-R132H, cells with endogenous IDH1 knocked down by targeted shRNA, and cells with a scrambled shRNA. This dataset also includes information on tumor type, IDH mutation status, and NAA and NAAG abundance expressed in nanograms per milligram protein for 26 tumor specimens from human glioma patients in the Tumor NAA_NAAG tab.